

# Bifurcations of the main auroral ring at Saturn: ionospheric signatures of consecutive reconnection events at the magnetopause

A. Radioti,<sup>1</sup> D. Grodent,<sup>1</sup> J.-C. Gérard,<sup>1</sup> S. E. Milan,<sup>2</sup> B. Bonfond,<sup>1</sup> J. Gustin,<sup>1</sup>  
and W. Pryor<sup>3</sup>

Received 16 March 2011; revised 25 August 2011; accepted 25 August 2011; published 10 November 2011.

[1] This work reports for the first time on bifurcations of the main auroral ring at Saturn observed with the UVIS instrument onboard Cassini. The observation sequence starts with an intensification on the main oval, close to noon, which is possibly associated with dayside reconnection. Consecutive bifurcations appear with the onset of dayside reconnection, between 11 and 18 magnetic local time, while the area poleward of the main emission expands to lower latitudes. The bifurcations depart with time from the main ring of emission, which is related to the open-closed field line boundary. The augmentation of the area poleward of the main emission following its expansion is balanced by the area occupied by the bifurcations, suggesting that these auroral features represent the amount of newly open flux and could be related to consecutive reconnection events at the flank of the magnetopause. The observations show that the open flux along the sequence increases when bifurcations appear. Magnetopause reconnection can lead to significant augmentation of the open flux within a couple of days and each reconnection event opens ~10% of the flux contained within the polar cap. Additionally, the observations imply an overall length of the reconnection line of ~4 hours of local time and suggest that dayside reconnection at Saturn can occur at several positions on the magnetopause consecutively or simultaneously.

**Citation:** Radioti, A., D. Grodent, J.-C. Gérard, S. E. Milan, B. Bonfond, J. Gustin, and W. Pryor (2011), Bifurcations of the main auroral ring at Saturn: ionospheric signatures of consecutive reconnection events at the magnetopause, *J. Geophys. Res.*, 116, A11209, doi:10.1029/2011JA016661.

## 1. Introduction

[2] Several studies suggest that the main auroral ring at Saturn is produced by field aligned currents and plasma precipitation associated with the solar wind magnetosphere interaction [e.g., Cowley *et al.*, 2004], similarly to the terrestrial aurora at Earth [e.g., Paschmann *et al.*, 2002]. Particularly, the analysis of in-situ Cassini data in comparison with auroral observations show that the quasi-continuous main ring of emissions is produced by magnetosphere-solar wind interaction, through the shear in rotational flow across the open closed field line boundary (OCFLB) [e.g., Bunce *et al.*, 2008; Talboys *et al.*, 2009]. The analysis of Hubble Space Telescope (HST) images of Saturn's southern FUV aurorae showed that the morphology of Saturn's aurora responds to the solar wind changes [Grodent *et al.*, 2005] and

its brightness and shape varies with time and often forms a spiral shape around the pole [Gérard *et al.*, 2004]. The spiral structures on newly opened and newly closed field lines are suggested to be the result of the combined action of reconnection and rotation [Cowley *et al.*, 2005]. The auroral morphology at Saturn is believed to be controlled by the balance between the magnetic field reconnection rate at the dayside magnetopause and the reconnection rate in the nightside tail [Badman *et al.*, 2005], similar to the Earth [Cowley and Lockwood, 1992; Milan *et al.*, 2003]. Observations [Gérard *et al.*, 2004, 2005] and theoretical studies [Bunce *et al.*, 2005] showed that bright FUV emissions at Saturn observed occasionally near noon are probably associated with reconnection occurring at the dayside magnetopause, similar to the "lobe cusp spot" at Earth Milan *et al.* [2000a]. Specifically it was proposed [Bunce *et al.*, 2005] that pulsed reconnection at Saturn at the low-latitude dayside magnetopause for northward directed Interplanetary Magnetic Field (IMF) is giving rise to pulsed twin-vortical flows in the magnetosphere and ionosphere in the vicinity of the OCFLB. For the case of southward IMF and high-latitude lobe reconnection pulsed twin-vortical flows, bi-polar field-aligned currents are expected and associated with auroral intensifications poleward of the OCFLB.

<sup>1</sup>Laboratoire de Physique Atmosphérique et Planétaire, Institut d'Astrophysique et de Géophysique, Université de Liège, Liège, Belgium.

<sup>2</sup>Department of Physics and Astronomy, University of Leicester, Leicester, U. K.

<sup>3</sup>Science Department, Central Arizona College, Coolidge, Arizona, USA.

[3] At Earth the reconnection process evolves in a transient manner with the occurrence of quasiperiodic bursts, known as flux transfer events (FTEs) [e.g., *Russell and Elphic*, 1979]. Ionospheric signatures of FTEs at Earth have been observed in the cusp region where they vary with the form of poleward-moving auroral structures [e.g., *Sandholt et al.*, 1986; *Milan et al.*, 2000b; *Sandholt and Farrugia*, 2007, 2008]. They are suggested to be associated with mixed magnetospheric and magnetosheath plasma connected to field lines of newly opened flux produced by reconnection [*Lockwood and Wild*, 1993]. The motion and plasma flow pattern, associated with these events is consistent with them being regions of newly opened flux, and thus are located within the polar cap, a region of the ionosphere threaded by open magnetic field lines. Specifically ultraviolet observations have shown bifurcations of the main Earth oval in the 14 to 16 magnetic local time (MLT) sector [*Milan et al.*, 2000b] and interpreted their poleward portion as an auroral signature of FTEs. In the present study we discuss similar auroral features at Saturn.

## 2. Bifurcations of the Main Auroral Emission

[4] The present work is based on auroral images taken with the UVIS instrument onboard Cassini. The narrow low-resolution slit of the FUV channel (11.5–191.2 nm) of the UVIS spectrometer provides 64 spatial pixels of 1 by 1.5 mrad along and across the slit [*Esposito et al.*, 2004]. All projections assume that the auroral emission peaks at 1100 km above the surface, in agreement with [*Gérard et al.*, 2009]. The projections display FUV emission restricted to the 120–163 nm range in order to maximize the contrast between the auroral signal and the day side planetary background (the reflected sunlight). The projected distance subtended by a pixel size changes proportionally with spacecraft altitude. Additionally, the overlap between projected pixels resulting from the combined motions of Saturn and Cassini is also considered in constructing the polar maps. In Figure 1 we present a sequence of polar projections of Saturn's northern aurora taken every ~15 minutes with the UVIS instrument on July 13 2008 (DOY 195) from 03:44 to 09:42 UT. The altitude of the spacecraft in this sequence decreases by ~0.5% from image to image. This effect is considered in the projections where all spatial pixels have been converted into a quadrilateral shape in the latitude-longitude map. The integration time of each record was 8 s and the region of interest, displayed in each image of Figure 1, was covered in ~6.6 min. During the sequence the sub-spacecraft planetocentric latitude increased from 32.6 to 37.7 deg and the spacecraft altitude, which is considered to be the distance from the surface, changed from 13.55 to 11.95  $R_S$ . Because of the relative high sub-spacecraft latitude, the limb brightening effect is limited and therefore no correction was applied. More details of the polar projection procedures are presented by *Grodent et al.* [2011].

[5] On image 3 an intensification on the main ring appears close to magnetic noon, marked feature a possibly a signature of reconnection at the low-latitude dayside magnetopause for the case of northward IMF as has been previously observed by HST [*Gérard et al.*, 2004, 2005] and theoretically predicted by *Bunce et al.* [2005]. On image 9,

a bifurcation of the main ring of emission appears to begin between ~11 and 14 MLT, marked feature b. From the present observations we cannot be sure that feature b is a separate feature, or if it is feature a that moves poleward with time. In the following we keep the notation b for this feature, without excluding the possibility that it is feature a in an evolved stage. Before feature b disappears, a second one, c in image 13, gradually detaches from the main emission and stays until the end of the sequence between ~14 and 18 MLT. Occasionally, we observe faint emission at the same latitude as the bifurcations that extend to earlier local times down to ~9h (images 13, 14, 18 and 19). These emissions are considered to be either continuation of feature b which is often too dim to be visible or a separate feature. The main oval emission expands with time to lower latitudes, a movement that is mainly evident for the bright dawn sector and for the dusk sector equatorward of features b and c. As the main ring progresses to lower latitudes, it creates a separation between the bifurcations and the main emission. This implies that the bifurcations are not part of the main ring and thus are related to the polar cap. The scale sizes of features b and c are  $\sim 10 \times 10^3$  by  $4 \times 10^3$  and  $6 \times 10^3$  by  $3 \times 10^3$  km in the azimuthal and meridional directions and each feature occupies an area of  $\sim 0.2$ – $0.33 \times 10^8$  km<sup>2</sup>. Independently, spot-like structures (marked with “s” on the images) appear on the dawn and dusk side, poleward of the main emission (images 10 to 24). Their size ranges from 5 to  $10 \times 10^6$  km<sup>2</sup>.

[6] Bifurcations of the main ring are regularly observed in the UVIS data set. We examined 37 data sets, some of which are obtained on the same date. In our analysis one date is considered as one case. Bifurcations of the main ring are observed in 6/16 dates, a fraction that corresponds to ~37% of the dates analyzed. Figure 2 shows three polar projections of Saturn's aurora taken on August 26 2008 (DOY 239), September 10 2008 (DOY 254) and January 21 2009 (DOY 021) with the UVIS instrument onboard Cassini. The first image is the sum of 3 sub-images of the northern hemisphere taken when the sub-spacecraft latitude was ranging from 59.5 to 54.6 deg and the altitude from 4.8 to 4.5  $R_S$ . The auroral region was scanned three times by performing continuous slews of the spacecraft in the direction perpendicular to the long-axis of the slit. The total image was covered in 72 min. The second image of Figure 2 is the sum of 2 sub images obtained in the southern hemisphere, when the spacecraft was at sub-spacecraft latitude ranging from 69 to 67.2 deg and the altitude from 5.7 to 5.9  $R_S$ . The auroral region was scanned twice by performing continuous slews of the spacecraft in the direction perpendicular to the long-axis of the slit and the total image was covered in 36 min. The third image of Figure 2 shows the aurora of the northern hemisphere taken when Cassini was at sub-spacecraft latitude 44.6 deg and altitude 14.5  $R_S$  and the region of interest was covered in ~13 min. The arrows in the three examples indicate the bifurcations of the main auroral ring in the afternoon auroral sector. Unfortunately, the present cases are not part of a long sequence and therefore one cannot discuss the temporal evolution of the bifurcations and the dynamics associated with these auroral forms. In the following section, we perform an in depth

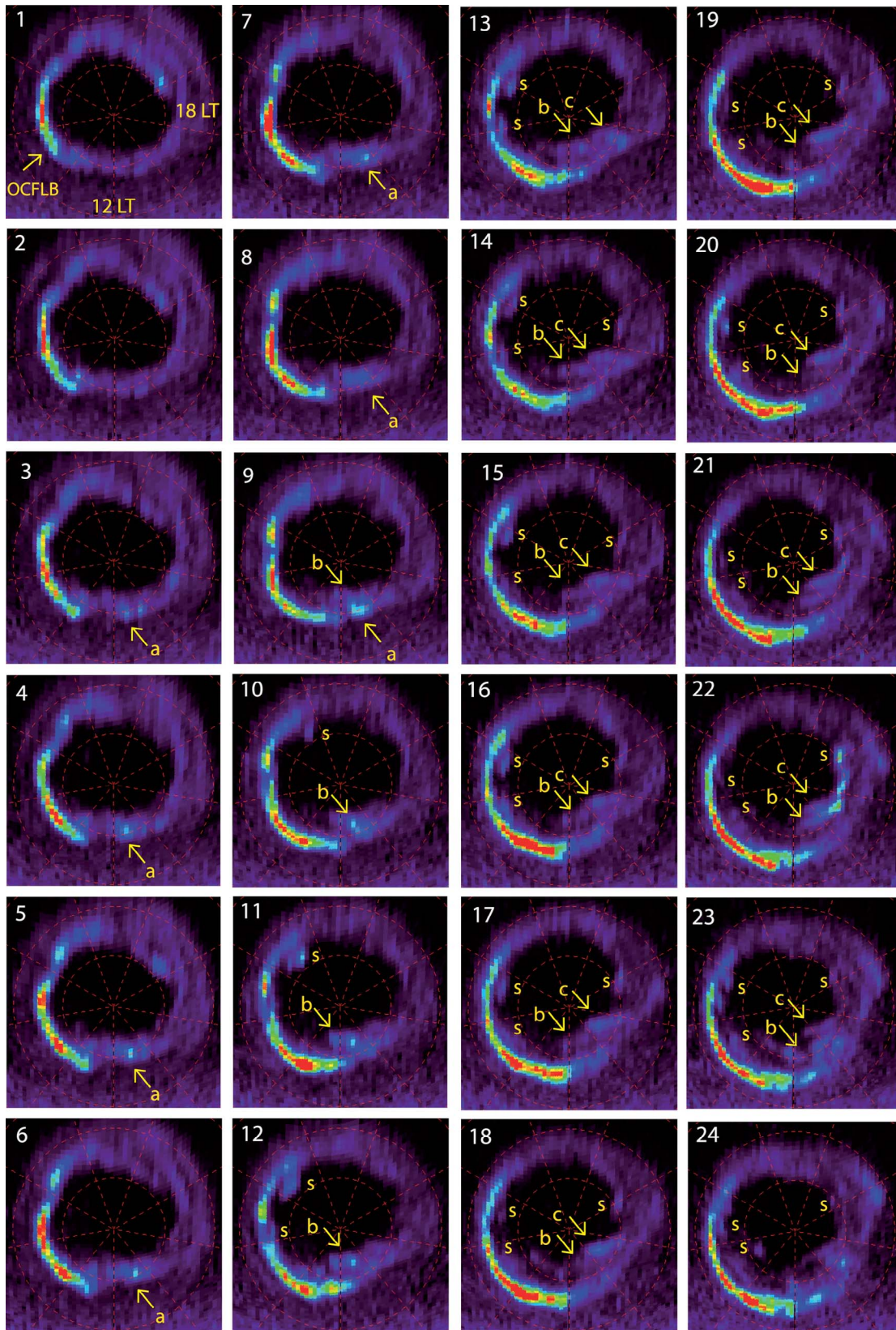


**Figure 1.** A sequence of polar projections of Saturn's northern aurora taken on July 13 2008 (DOY 195) from 03:44 to 09:42 UT with the UVIS instrument onboard Cassini. Noon is to the bottom and dusk to the right. Arrows indicate the OCFLB and several features under discussion: a, an intensification of the main ring; b and c, bifurcations of the main ring which evolve to auroral arcs; and s, transient spot-like structures.



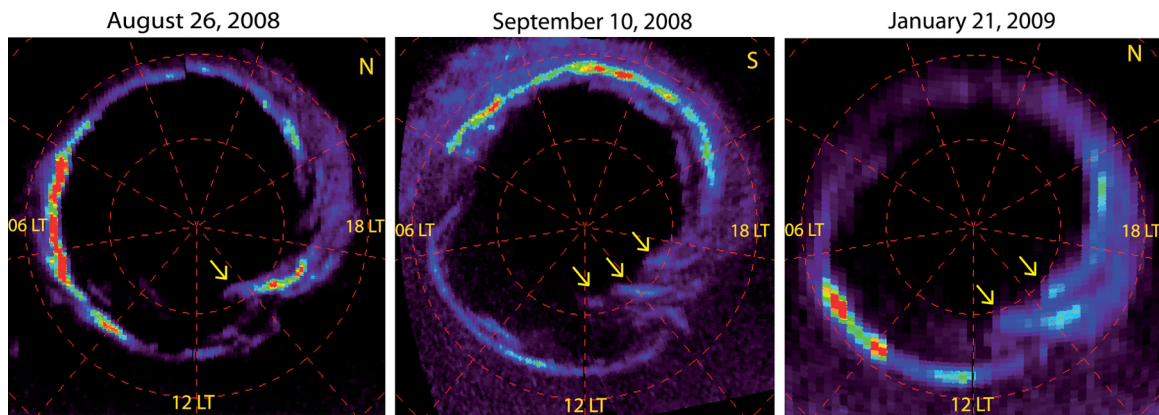


**Figure 2.** Polar projections of Saturn’s northern and southern aurora taken on August 26 2008 (DOY 239), September 10 2008 (DOY 254), and January 21 2009 (DOY 021) with the UVIS instrument onboard Cassini. The arrows indicate the bifurcations observed in the afternoon sector.

analysis of the bifurcations observed on July 13, 2008 shown in the sequence of Figure 1.

### 3. Ionospheric Signatures of Consecutive Reconnection Events at Saturn

[7] We suggest that the bifurcations reported here are related to consecutive reconnection events at the magnetopause. The sketch in Figure 3 illustrates the concept of reconnection near Saturn’s magnetopause (adapted to Saturn, from *Lockwood and Wild [1993]*). Reconnection at the “x point” produces a pair of bubbles of mixed magnetospheric and magnetosheath plasma. The bubbles are connected to field lines of newly opened flux produced by the reconnection. The ionospheric footprint of the newly open field lines is indicated on the sketch.

[8] If the auroral features under study are the ionospheric signatures of consecutive reconnection events at the magnetopause of Saturn, they should represent the total magnetic flux opened during dayside reconnection processes. In order to estimate the location of the OCFLB we use a cut-off intensity, which corresponds to an average value of the day and night glow emission. The day and night glow emission used as threshold is selected manually on each image. This method is slightly different from previous studies [*Badman et al., 2005*] which determined the boundary by looking for a sharp increase in the emission intensity between the polar region and the auroral zone. In some local time regions where there are no auroral features distinguishable the authors estimated the boundary by extrapolating from earlier and later magnetic local times. In the present study, we define the region, which we term the “dim polar region”, as the region within which the emission intensity does not exceed the level of day and night glow background emissions. Our threshold does not depend on the maximum auroral intensity along a longitudinal cut, which is changing significantly with local time. The Cassini UVIS data set, because of the instrument’s observing geometry and low sensitivity threshold, allows someone regularly to define the boundary at all local times. For clarity, we consider that each image represents an instantaneous snapshot of the aurora even though, as mentioned before, each image of this sequence is covered within  $\sim 6.6$  min. This simplifying assumption does not affect significantly our

analysis since the features under study, the bifurcations, are observed to last a couple of hundreds of minutes and do not evolve significantly within timescales of few minutes. We assume that the main ring of emission is associated with the OCFLB, as several studies have previously shown [e.g., *Bunce et al., 2008; Talboys et al., 2009*], consequently the region poleward of it should represent the region of the open magnetic flux, which is commonly associated with the polar cap. Accordingly, auroral features that are observed inside the polar cap are at the foot of open field lines (see sketch in Figure 3). In the following we consider that the bifurcations reported here represent open flux. The “dim polar region” corresponds to the polar cap with the exception of the case where emission features are observed poleward of the main ring which could be related to open flux such as the bifurcations. In such cases the polar cap extends beyond the “dim polar region” and covers the area of the bifurcations.

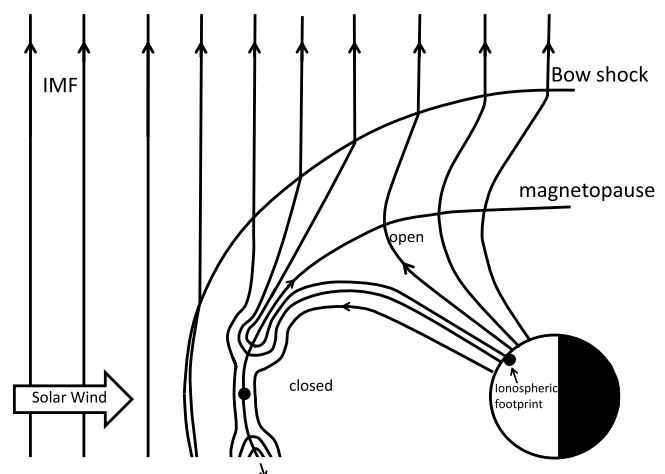


**Figure 3.** Schematic illustration of reconnection at Saturn’s magnetopause (adapted from *Lockwood and Wild [1993]*). The dot marks the position of the reconnection site. Closed field lines are converted to open. A pair of bubbles of mixed magnetospheric and magnetosheath plasma is produced and moves away from the reconnection site, as shown by the arrows. The ionospheric footprint of the newly open field lines is indicated.

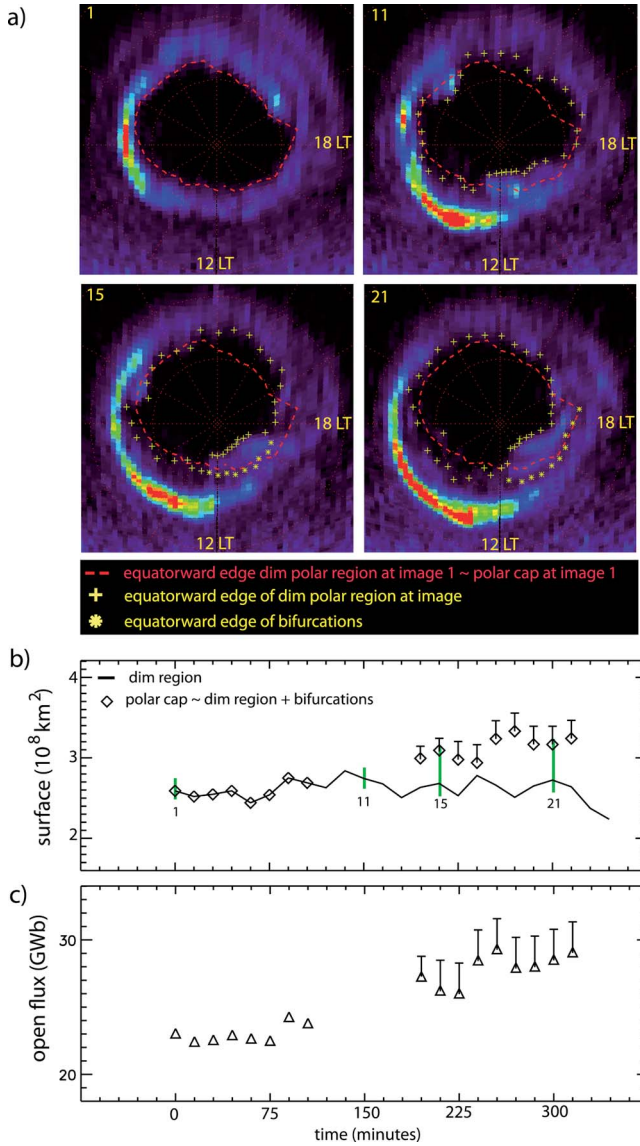


**Figure 4.** (a) Selected polar projections of the sequence shown in Figure 1. The red dashed line indicates the polar cap at image 1 and it is over plotted on the rest of images for comparison. The yellow crosses at images 11, 15 and 21 indicate the equatorward edge of the dim polar region and the star symbols the equatorward edge of the auroral arcs. (b) Area of the dim polar region (solid line) of all images of Figure 1 as a function of time starting at 03:44 UT. Total area of the dim polar region and the bifurcations (diamonds) for the cases where there is a clear separation between the main ring and the bifurcations. The areas of the images shown in Figure 4a are marked by green lines in Figure 4b. (c) Open flux of the images of Figure 1 as a function of time. The error bars in Figures 4b and 4c indicate the maximum discrepancy in the polar cap size and open flux if we consider that spots “s” are related to open flux.

[9] We define the “dim polar region” for all the images of Figure 1. Figure 4 shows four selected polar projections on top of which we plot the dim region. The dim polar region (red dashed line) on image 1 (Figure 4) is considered to correspond to the polar cap size since there are not bifurca-

tions or spot-like structures poleward of it, which could be related to open flux. The yellow crosses on the aurora at images 11, 15 and 21 indicate the equatorward edge of the dim polar region. The star symbols in Figure 4 indicate the equatorward edge of the bifurcations, while their poleward edge is defined by the dim polar region. The polar cap size of image 1 is over-plotted on the other three images for comparison and it shows that the poleward boundary of the main ring of emission moves to lower latitudes with time, therefore suggesting the addition of new open flux to the pre-existing open flux of the polar cap. Particularly, from image 1 to 21 the boundary is expanded in latitude by a range of 1 to 2.12 deg within 00–06 LT, 1 to 2.9 deg within 06–12 LT, –1.2 to 1.65 within 12–18 LT and –1.3 to 2.19 within 18–24 LT. The negative values denote a local contraction of the oval which occurs only for a couple of isolated cases (see image 21 in Figure 4). The expansion of the poleward boundary of the main emission, which approximates here the polar cap size should not be confused with the oscillations of the main ring of emissions [Nichols *et al.*, 2008]. The latter were determined from the tracing of the equatorward (not the poleward) boundary and are related to a shift of the center of the oval by 1.5 deg in latitude, rather than an expansion at almost all local times. Figure 4b shows that the dim polar region surface is changing with time and ranges between  $2.23$  to  $2.83 \times 10^8 \text{ km}^2$ . Assuming that the bifurcations represent open flux as justified above, the sum of the dim polar region surface and that of the bifurcations approximates the polar cap size. It ranges between  $2.4$  and  $3.35 \times 10^8 \text{ km}^2$  (Figure 4b, diamonds) and increases with the appearance of the bifurcations. The relatively uniform size of the dim region indicates that the increase of the polar cap surface following its expansion is equal to the area occupied by the bifurcations. This is an indication that the auroral features reported here probably represent the amount of newly open flux and thus could be related to consecutive reconnection events at the magnetopause. Their size is estimated to be of the order of  $0.2\text{--}0.3 \times 10^8 \text{ km}^2$  each, which represents the area of the polar cap created by each event.

[10] We estimate the amount of open flux contained within the polar cap region with the flux function  $F(r, \theta)$ , described by Cowley and Bunce [2003], which is related to the field components by  $\mathbf{B} = (1/r \sin \theta) \nabla F \times \hat{\varphi}$ , where  $F$  is constant on a field line:

$$F(r, \theta) = R_S^2 \sin^2 \theta \left[ g_1^0 \frac{R_S}{r} + \frac{3}{2} g_2^0 \cos \theta \left( \frac{R_S}{r} \right)^2 + \frac{1}{2} g_3^0 \cdot (5 \cos^2 \theta - 1) \left( \frac{R_S}{r} \right)^3 \right] \quad (1)$$

[11] The function is employed in spherical polar coordinates, with  $r$  the distance from the center of the planet,  $\theta$  the co-latitude angle measured from the north pole and  $\varphi$  the azimuthal angle. The absolute value of  $F$  has been fixed by taking  $F = 0$  on the magnetic axis. The coefficients of the Saturn-Pioneer-Voyager (SPV) model [Davis and Smith, 1990] are used:  $g_1^0 = 21160$ ,  $g_2^0 = 1560$ , and  $g_3^0 = 2320 \text{ nT}$  for a conventional Saturn radius of  $R_S = 60,330 \text{ km}$ . We consider that the amount of magnetic flux threading any surface bounded by a ring of radius, defined by the distance  $r$  from the center of the planet at co-latitude  $\theta$  is  $\Phi = 2\pi F(r, \theta)$ .

We divide the polar cap area on the polar projections into 36 longitudinal sectors, each  $10^\circ$  wide and similarly to *Badman et al.* [2005] we estimate the amount of the magnetic flux using:

$$\Phi = \Delta\varphi \sum_{n=1}^{36} F(R(\theta_n), \theta_n), \quad (2)$$

where  $\theta_n$  is the co-latitude of the boundary in longitude sector  $n$  and  $R(\theta_n)$  is the distance from the center of the planet which defines the surface containing the auroral emissions at that co-latitude. The surface is assumed to be an ellipsoid of revolution about the spin axis with an equatorial radius  $R_e$  and a polar radius  $R_p$ :

$$R(\theta) = \frac{R_e}{(1 + \varepsilon \cos^2 \theta)^{1/2}} \quad (3)$$

where  $\varepsilon = (\frac{R_e}{R_p})^2 - 1$ ,  $R_e = 61368$  km,  $R_p = 55464$  km and  $\varepsilon \approx 0.22$ , assuming that the peak auroral emissions lies  $\sim 1100$  km above the 1 bar reference ellipsoid of the planet [e.g., *Grodent et al.*, 2005; *Gérard et al.*, 2009].

[12] Figure 4c shows the open flux variations for the sequence presented in Figure 1. For images 9 to 13 the open flux could not be estimated because the bifurcations are not well separated from the main emission and there is no clear boundary between the main emission and the open flux. The estimated open flux at the beginning of the sequence is 22–23 GWb and at the end it reaches values up to 29 GWb. For images 14 to 22 (from 195 to 315 min) the open flux changes from 27.28 to 29.09 GWb within 120 min, giving rise to an augmentation of the flux of 1.81 GWb which for the given time corresponds to voltage (flux rate) of 250 kV. *Badman et al.* [2005] analyzed daily HST images and showed that the open flux at Saturn is between  $\sim 15$  and 50 GWb over a period of a month, while the derived voltage ranges from  $\sim 10$  to 250 kV during the same period. The authors compared their results with theoretical calculation of the average magnetopause and tail reconnection voltages at 1 min resolution for solar wind conditions this given period, following *Jackman et al.* [2004], and showed that voltages range between  $\sim 10$  to 400 kV (and for specific solar wind conditions up to 700 kV). Our results demonstrate that magnetopause reconnection can lead to significant augmentation of the open flux within a couple of hours. We estimate that each event at the end of the sequence opened  $\sim 10\%$  of the flux contained in the polar cap, similar to the fractions estimated for FTEs at Earth,  $\sim 10\%$  in the work of *Milan et al.* [2000b] and  $\sim 3\%$  in the work of *Lockwood et al.* [1990].

[13] Additionally, the consecutive bifurcations of the main ring between 11 and 18 MLT appear within  $\sim 60$  min each, on the same order of magnitude with the 20–30 min reconnection interpulse period estimated for Saturn [*Bunce et al.*, 2005], in analogy with the FTEs seen at Earth. The bifurcations appear to detach of the main emission at different local times, implying that the reconnection site moves duskward. The main ring of emissions at Saturn expands to lower latitudes and the bifurcations gradually separate from the main emission. This is consistent with the combined effect of magnetic tension and antisunward magnetosheath flow which force the newly reconnected field lines to move away from the subsolar magnetopause reconnection site. Its newly open flux is then

assimilated with the preexisting open flux of the polar cap. Additionally, our observations are consistent with theoretical studies about ongoing dayside magnetopause reconnection according to which auroral brightening is expected in the pre-noon sector and dimming of the emission in the post-noon and nightside sector [*Cowley et al.*, 2004]. Finally, the present auroral features morphologically resemble the bifurcations observed at Earth, which are characterized by their transient nature and location in the post-noon sector poleward of the OCFLB and associated with FTEs [*Milan et al.*, 2000b].

[14] The spot-like structures such as those appearing on the dawn side poleward of the main emission (marked with s on images 10 to 24) are located equatorward of the dim polar region and thus are not included in the estimation of the polar cap surface. There is no evidence that they could be involved in the same dynamics as the bifurcations in the post-noon sector. Their size ranges from  $\sim 5$  to  $10 \times 10^6$  km<sup>2</sup>, one order of magnitude less than the size of the bifurcations ( $2$  to  $3 \times 10^7$  km<sup>2</sup>). If they are associated with open flux then  $5$  to  $10 \times 10^6$  km<sup>2</sup> should be added to the polar cap size for each spot. The upper error bars in Figures 4b and 4c show the maximum discrepancy in the polar cap size and open flux if we consider that spots s are related to open field lines. We consider that each spot adds  $7.5 \times 10^6$  km<sup>2</sup> and 0.75 GWb to the size of the polar cap and the open flux, respectively. Additionally, previous studies based on HST data reported the presence of transient features in the dusk auroral sector and associated them with regions of injected plasma [*Radioti et al.*, 2009]. The HST observations, though, did not reveal any auroral feature resembling the bifurcations of the main emission initiating close to noon presented in the current study and therefore we cannot establish an association between the injected cloud discussed by *Radioti et al.* [2009] with a signature of reconnection event at the magnetopause.

[15] The present auroral observations provide an estimate of the instantaneous length of the reconnection line, which may be used as a proxy of the efficiency of coupling between the IMF and magnetosphere, a quantity that can be hardly accessed by in-situ spacecraft measurements. The bifurcations take place instantaneously between  $\sim 11$  and 18 MLT, but they protrude from a confined region that covers  $\sim 4$  hours of local time, implying an overall length of the reconnection line of  $\sim 4$  hours of local time ( $\sim 60^\circ$ ). These observations also suggest that dayside reconnection at Saturn can occur at several positions on the magnetopause consecutively or simultaneously and the reconnection lines follow each other as they sweep along the flank of the magnetopause, as suggested for the Earth [*Milan et al.*, 2000b]. Similarly, recent auroral observations at Jupiter demonstrated that quasiperiodic auroral flares could be related to pulsed reconnection at the dayside magnetopause and their fast propagation was interpreted as the relocation of the reconnection site with time [*Bonfond et al.*, 2011].

[16] Voyager observations showing reconnection signatures at Saturn's magnetopause [*Huddleston et al.*, 1997] suggest that bursty reconnection such as the FTEs at Earth [*Russell and Elphic*, 1979] is not a significant mechanism at Saturn. The high magnetosonic Mach numbers which are reached close to Saturn decrease the reconnection efficiency and therefore dayside reconnection at Saturn is not expected to be significant [*Scurry and Russell*, 1991]. However, a recent study [*Grocott et al.*, 2009] based on radar observations of the ionospheric electric field showed that there is no evidence for significant

reduction in the magnetopause reconnection rate associated with high magnetosonic Mach numbers, contradicting the results of *Scurry and Russell* [1991]. Additionally, Cassini plasma and magnetic field observations revealed signatures of reconnection at Saturn's magnetopause [*McAndrews et al.*, 2008]. On the basis of the calculation of the reconnection voltage, the authors concluded that magnetopause reconnection is not an uncommon mechanism at Saturn and plays a role in the magnetospheric dynamics. Additionally, previous auroral observations [*Gérard et al.*, 2004, 2005] and theoretical studies [*Bunce et al.*, 2005] suggested the presence of reconnection at the dayside magnetopause. The present study shows that bifurcations in Saturn's auroral ring are possibly associated with open magnetic flux and thus could be related to consecutive reconnection events near the magnetopause. A preliminary statistical analysis (~37% of the present UVIS data set show bifurcations) indicates that consecutive reconnection events in the magnetopause might not be a frequent mechanism at Saturn but it is not a negligible process.

#### 4. Summary and Conclusions

[17] The present work reports for the first time on observations of bifurcations of the main auroral ring at Saturn and suggests an association with consecutive reconnection events at the magnetopause. The features under study similarly to the ionospheric signatures of FTEs at Earth [*Milan et al.*, 2000b] have a transient nature and are located on the post-noon sector poleward of the OCFLB. The consecutive bifurcations of the main ring appear between 11 and 18 MLT, within ~60 min each, a timescale of the same order of magnitude with the 20–30 minutes reconnection interpulse period estimated for Saturn [*Bunce et al.*, 2005], in analogy with the FTEs seen at Earth. The auroral features depart from the main ring of emissions (OCFLB) as expected for the ionospheric footprint of each newly reconnected field lines moving away from the subsolar magnetopause reconnection site. The newly open flux is assimilated with the pre-existing open flux of the polar cap. The augmentation of the area poleward of the main emission following its expansion is balanced by the area occupied by the bifurcations, supporting the scenario that these auroral features represent the amount of newly open flux and therefore could be related to consecutive reconnection events at the magnetopause. The open flux increases along the sequence when the bifurcations appear and magnetopause reconnection can lead to significant augmentation of the open flux within a couple of days. Each reconnection event opens ~10% of the flux contained within the polar cap, similar to the fraction estimated for FTEs at Earth. The present auroral observations imply an overall length of the reconnection line of 4 hours of local time (~60°). This study also suggests that dayside reconnection at Saturn can occur consecutively or simultaneously at several locations on the magnetopause and the reconnection lines follow each other as they sweep along the flank of the magnetopause.

[18] **Acknowledgments.** This work is based on observations with the UVIS instrument onboard the NASA/ESA Cassini spacecraft. The research was supported by PRODEX Program managed by the European Space Agency in collaboration with the Belgian Federal Science Policy Office. A.R., D.G. and J.-C.G. are funded by the Belgian Fund for Scientific Research

(FNRS). The work in this paper was discussed during a meeting of the International Team on Planetary Magnetotails at the International Space Science Institute.

[19] Masaki Fujimoto thanks the reviewers for their assistance in evaluating this paper.

#### References

- Badman, S. V., E. J. Bunce, J. T. Clarke, S. W. H. Cowley, J.-C. Gérard, D. Grodent, and S. E. Milan (2005), Open flux estimates in Saturn's magnetosphere during the January 2004 Cassini-HST campaign, and implications for reconnection rates, *J. Geophys. Res.*, **110**, A11216, doi:10.1029/2005JA011240.
- Bonfond, B., M. F. Vogt, J.-C. Gérard, D. Grodent, A. Radioti, and V. Coumans (2011), Quasi-periodic polar flares at Jupiter: A signature of pulsed dayside reconnections?, *Geophys. Res. Lett.*, **38**, L02104, doi:10.1029/2010GL045981.
- Bunce, E. J., S. W. H. Cowley, and S. E. Milan (2005), Interplanetary magnetic field control of Saturn's polar cusp aurora, *Ann. Geophys.*, **23**, 1405.
- Bunce, E. J., et al. (2008), Origin of Saturn's aurora: Simultaneous observations by Cassini and the Hubble Space Telescope, *J. Geophys. Res.*, **113**, A09209, doi:10.1029/2008JA013257.
- Cowley, S. W. H., and E. J. Bunce (2003), Corotation-driven magnetosphere-ionosphere coupling currents in Saturn's magnetosphere and their relation to the auroras, *Ann. Geophys.*, **21**, 1691–1707.
- Cowley, S. W. H., and M. Lockwood (1992), Excitation and decay of solar wind-driven flows in the magnetosphere-ionosphere system, *Ann. Geophys.*, **10**, 103–115.
- Cowley, S. W. H., E. J. Bunce, and R. Prangé (2004), Saturn's polar ionospheric flows and their relation to the main auroral oval, *Ann. Geophys.*, **22**, 1379–1392.
- Cowley, S. W. H., S. V. Badman, E. J. Bunce, J. T. Clarke, J.-C. Gérard, D. Grodent, C. M. Jackman, S. E. Milan and T. K. Yeoman (2005), Reconnection in a rotation-dominated magnetosphere and its relation to Saturn's auroral dynamics, *J. Geophys. Res.*, **110**, A02201, doi:10.1029/2004JA010796.
- Davis, L., Jr., and E. J. Smith (1990), A model of Saturn's magnetic field based on all available data, *J. Geophys. Res.*, **95**, 15,257.
- Esposito, L. W., et al. (2004), The Cassini Ultraviolet Imaging Spectrograph Investigation, *Space Sci. Rev.*, **115**, 299–361.
- Gérard, J.-C., D. Grodent, J. Gustin, A. Saglam, J. T. Clarke, and J. T. Trauger (2004), Characteristics of Saturn's FUV aurora observed with the Space Telescope Imaging Spectrograph, *J. Geophys. Res.*, **109**, A09207, doi:10.1029/2004JA010513.
- Gérard, J.-C., E. J. Bunce, D. Grodent, S. W. H. Cowley, J. T. Clarke, and S. V. Badman (2005), Signature of Saturn's auroral cusp: Simultaneous Hubble Space Telescope FUV observations and upstream solar wind monitoring, *J. Geophys. Res.*, **110**, A11201, doi:10.1029/2005JA011094.
- Gérard, J.-C., B. Bonfond, J. Gustin, D. Grodent, J. T. Clarke, D. Bisikalo, and V. Shematovich (2009), Altitude of Saturn's aurora and its implications for the characteristic energy of precipitated electrons, *Geophys. Res. Lett.*, **36**, L02202, doi:10.1029/2008GL036554.
- Grocott, A., S. V. Badman, S. W. H. Cowley, S. E. Milan, J. D. Nichols, and T. K. Yeoman (2009), Magnetosonic Mach number dependence of the efficiency of reconnection between planetary and interplanetary magnetic fields, *J. Geophys. Res.*, **114**, A07219, doi:10.1029/2009JA014330.
- Grodent, D., J.-C. Gérard, S. W. H. Cowley, E. J. Bunce, and J. T. Clarke (2005), Variable morphology of Saturn's southern ultraviolet aurora, *J. Geophys. Res.*, **110**, A07215, doi:10.1029/2004JA010983.
- Grodent, D., J. Gustin, J.-C. Gérard, A. Radioti, B. Bonfond, and W. R. Pryor (2011), Small-scale structures in Saturn's ultraviolet aurora, *J. Geophys. Res.*, **116**, A09225, doi:10.1029/2011JA016818.
- Huddleston, D. E., C. T. Russell, G. Le, and A. Szabo (1997), Magnetopause structure and the role of reconnection at the outer planets, *J. Geophys. Res.*, **102**, 24,289–24,004.
- Jackman, C. M., N. Achilleos, E. J. Bunce, S. W. H. Cowley, M. K. Dougherty, G. H. Jones, S. E. Milan, and E. J. Smith (2004), Interplanetary magnetic field at 79 AU during the declining phase of the solar cycle and its implications for Saturn's magnetospheric dynamics, *J. Geophys. Res.*, **109**, A11203, doi:10.1029/2004JA010614.
- Lockwood, M., and M. N. Wild (1993), On the quasi-periodic nature of magnetopause flux transfer events, *J. Geophys. Res.*, **98**(A4), 5935–5940.
- Lockwood, M., S. W. H. Cowley, and M. P. Freeman (1990), The excitation of plasma convection in the high-latitude ionosphere, *J. Geophys. Res.*, **95**, 7961–7972.
- McAndrews, H. J., C. J. Owen, M. F. Thomsen, B. Lavraud, A. J. Coates, M. K. Dougherty, and D. T. Young (2008), Evidence for reconnection at Saturn's magnetopause, *J. Geophys. Res.*, **113**, A04210, doi:10.1029/2007JA012581.



- Milan, S. E., M. Lester, S. W. H. Cowley, and M. Brittnacher (2000a), Dayside convection and auroral morphology during an interval of northward interplanetary magnetic field, *Ann. Geophys.*, **18**, 436–444.
- Milan, S. E., M. Lester, S. W. H. Cowley, and M. Brittnacher (2000b), Convection and auroral response to a southward turning of the IMF: Polar UVI, CUTLASS, and IMAGE signatures of transient magnetic flux transfer at the magnetopause, *J. Geophys. Res.*, **105**(A7), 15,741–15,755.
- Milan, S. E., M. Lester, S. W. H. Cowley, K. Oksavik, M. Brittnacher, R. A. Greenwald, G. Sofko, and J.-P. Villain (2003), Variations in polar cap area during two substorm cycles, *Ann. Geophys.*, **21**, 1121–1140.
- Nichols, J. D., J. T. Clarke, S. W. H. Cowley, J. Duval, A. J. Farmer, J.-C. Gérard, D. Grodent, and S. Wannawichian (2008), Oscillation of Saturn's southern auroral oval, *J. Geophys. Res.*, **113**, A11205, doi:10.1029/2008JA013444.
- Paschmann, G., S. Haaland, and R. Treumann (2002), Auroral plasma physics, *Space Sci. Rev.*, **103**, 475.
- Radioti, A., D. Grodent, J.-C. Gérard, E. Roussos, C. Paranicas, B. Bonfond, D. G. Mitchell, N. Krupp, S. Krimigis, and J. T. Clarke (2009), Transient auroral features at Saturn: Signatures of energetic particle injections in the magnetosphere, *J. Geophys. Res.*, **114**, A03210, doi:10.1029/2008JA013632.
- Russell, C. T., and R. C. Elphic (1979), ISEE observations of flux transfer events at the dayside magnetopause, *Geophys. Res. Lett.*, **6**, 33–36.
- Sandholt, P. E., and C. J. Farrugia (2007), Poleward moving auroral forms (PMAFs) revisited: Responses of aurorae, plasma convection and Birke-land currents in the pre-and postnoon sectors under positive and negative IMF By conditions, *Ann. Geophys.*, **25**, 1629–1652.
- Sandholt, P. E., and C. J. Farrugia (2008), The role of external triggers in flow shear arcs in the dayside auroral, *Ann. Geophys.*, **26**, 2159–2177.
- Sandholt, P. E., C. S. Deehr, A. Egeland, B. Lybekk, and R. Viereck (1986), Signatures in the dayside aurora of plasma transfer from the magnetosheath, *J. Geophys. Res.*, **91**, 10,063–10,079.
- Scurry, L., and C. T. Russell (1991), Proxy studies of energy transfer to the magnetosphere, *J. Geophys. Res.*, **96**, 9541–9548.
- Talboys, D. L., C. S. Arridge, E. J. Bunce, A. J. Coates, S. W. H. Cowley, and M. K. Dougherty (2009), Characterization of auroral current systems in Saturn's magnetosphere: High-latitude Cassini observations, *J. Geophys. Res.*, **114**, A06220, doi:10.1029/2008JA013846.
- B. Bonfond, J.-C. Gérard, D. Grodent, J. Gustin, and A. Radioti, Laboratoire de Physique Atmosphérique et Planétaire, Institut d'Astrophysique et de Géophysique, Université de Liège, B-4000 Liège, Belgium. (a.radioti@ulg.ac.be)
- S. E. Milan, Department of Physics and Astronomy, University of Leicester, University Road, Leicester LE1 7RH, U. K.
- W. Pryor, Science Department, Central Arizona College, Coolidge, AZ 85128, USA.